

Quantum Field as a Quantum Cellular Automaton I: the Dirac free evolution in one dimension

Alessandro Bisio,^{*} Giacomo Mauro D’Ariano,[†] and Alessandro Tosini[‡]
*Dipartimento di Fisica dell’Università di Pavia, via Bassi 6, 27100 Pavia and
Istituto Nazionale di Fisica Nucleare, Gruppo IV, via Bassi 6, 27100 Pavia*

It is shown how a quantum cellular automaton can describe very precisely the Dirac evolution, without requiring Lorentz covariance. The automaton is derived with the only assumptions of minimal dimension and parity and time-reversal invariance. The automaton extends the Dirac field theory to the Planck and ultrarelativistic scales. The Dirac equation is recovered in the usual particle physics scale of inertial mass and momenta. In this first paper the simplest case of one space dimension is analyzed. We provide a technique to derive an analytical approximation of the evolution of the automaton in terms of a momentum-dependent Schrödinger equation. Such approximation works very well in all regimes, including ultrarelativistic and Planckian, for the typical smooth quantum states of field theory with limited bandwidth in momentum. Finally we discuss some thought experiments for falsifying the existence of the automaton at the Planck scale.

PACS numbers: 11.10.-z, 03.70.+k, 03.67.Ac, 03.67.-a, 04.60.Kz

I. INTRODUCTION

Quantum Field Theory (QFT) is the most detailed description of the dynamics of physical systems available. Its predictions are extremely accurate, and have been tested in a countless number of experiments. Despite its impressive predictive power, QFT is affected by a number of conceptually relevant issues, including all problems arising from the continuum, localizability, causality violation, and quantization (for a review, see Refs. [1–5]). The main framework is made of recipes that are validated a posteriori, e.g. the quantization rules, both the canonical and the Feynman’s path integral, the former being affected by the ordering issue, the latter being based on a mathematically undefined notion. In practice a quantized theory is first formulated, and then checked a posteriori if it is renormalizable, otherwise it is discarded. This process has been one of the main theory-sieve in the formulation of the so-called Standard Model [6], the worldwide collaborative effort that succeeded in explaining a wide variety of experimental results, to the extent of being regarded as a “theory of almost everything”. However, the price to pay is the limited validity of the theory, which does not accommodate gravity.

The issue of localizability [1, 7] in QFT—the essential ingredient of the particle concept—is widely considered one of the most severe, since it prevents the formulation of a rigorous quantum theory of measurement for fields. It is also the main hallmark of the unsolvable tension between relativity and quantum theory, as for e.g. the boost-induced delocalization of Newton-Wigner states [8]. This is also another side of the causality violation due to the Hamiltonian description, which leads

to the wave-function superluminal tails [9].

There is no easy way for curing all the issues plaguing QFT, if not through a reconsideration of its very foundations. It is common opinion that the continuum description of space-time is the source of the problem, and that at some very small scale—the Planck scale—the description should be taken discrete. This is the mainstream philosophy of the approaches to quantum space-time [10, 11], of loop quantum-gravity [12–14], and, in some way, of the causal set approach [15]. The discreteness of the Planck-scale has also the consequence that Lorentz covariance and all symmetries of QFT are no longer valid, and are recovered at the Fermi scale [16–18]. Recently, potential experimental tests of Planck-scale phenomenology have been proposed by several authors [19–22].

A description of the quantum field as a quantum cellular automaton (QCA) represents a logically coherent way of tackling the Planck scale discreteness with minimal assumptions. Compared to other approaches, the QCA is motivated by a list of reasons. First: it relaxes the tension between quantum theory and relativity, since it does not need relativity, which in turn is emergent from the former. Second: it is quantum *ab-initio*, without the need of quantization rules. Third: it is free from all the problems arising from the continuum, and doesn’t suffer violations of causality.

A first classical automaton description for the Dirac field evolution is hidden in the nonstandard analysis formulation of the path-integral of Nakamura [23], where the “infinitesimal” plays the role of the Planck length. Then, the word “automaton” first appeared in relation to relativistic field-theory in the pioneering work of Bialynicki-Birula [24], where the automaton describes a discretization of the Weyl differential equation. The automaton is synthesized by a unitary matrix, but it is still a classical one, representing an updating rule on a lattice of classical variables. The possibility of using automata for describing the evolution of classical relativistic fields also emerged in the context of lattice-gas simulations, espe-

^{*}alessandro.bisio@unipv.it

[†]dariano@unipv.it

[‡]alessandro.tosini@unipv.it

cially in the seminal work of Meyer [25], where a notion of “field automaton” first appeared, and in the papers of Yepez [26]. In all cases, however, the automata are classical ones, and are devised as simulation tools for a discretized path-integral approach.

Recently the quantum cellular automaton has been proposed as a minimal-assumption extension to the Planck and ultrarelativistic scales of QFT [27–30]. A Dirac automaton in one-dimension has been derived without imposing Lorentz covariance, starting from principles of information-theoretical nature (for a nontechnical review see Ref.[31]). As we will see in this paper, the automaton is described by a simple 2×2 matrix: however, despite its simplicity, the QCA describes a very rich physical phenomenology, leading to unexpected interesting predictions, e.g. it anticipates an upper bound to the inertial mass of the Dirac field [29], as a simple consequence of unitarity of quantum evolution, without invoking black-hole arguments from general-relativity. Moreover, the automaton framework even allows to redefine fundamental physical notions and physical constants in an informational way [28, 30].

The quantum cellular automaton represents an extension of QFT, in the sense that it describes also localized states and measurements that are not manageable by QFT, giving a unified description of the field dynamics at all scales, ranging from the Planck, ultrarelativistic to the usual particle-physics scale.

In this work we provide a thorough study of the physics emerging from the Dirac automaton in one space-dimension of Ref. [29], showing how the Dirac dynamics is perfectly recovered at the Fermi scale, though relativistic covariance and other symmetries are violated at the Planck and ultrarelativistic ones (a Dirac quantum automaton has also been derived recently for space dimension $d = 2, 3$, and will be the object of the next publication [32] of this series).

The QCA generalizes the notion of cellular automaton of von Neumann [33] to the quantum case. The earliest appearance of the notion of QCA in the literature dates back to 1982 from R. Feynman [34]. The first QCA as we know it nowadays has been introduced in Ref. [35]. In the following literature the QCA has been mostly a computer-science object of investigation, especially in the field of quantum information, with interesting general mathematical results [36–38]. However, the QCA has never been used as a theoretical framework for physics, as e.g. field theory, as we will do in this paper.

The classical cellular automaton consists of a regular lattice, whose sites can be in a finite number of states (e.g. on and off) along with a rule that updates the state from “time” t to $t + 1$. This rule must be *local*, namely the state at site x at time $t + 1$ depends only on the states of a finite set of neighbouring sites at time t . In the quantum version, the sites of the lattice are quantum systems interacting unitarily with a finite set of neighbouring systems. In the present context, the lattice

is a Planck scale version of the notion of space. The metric corresponds to counting systems along the lattice, and the conversion from counting to the usual metric is given by a unit length which is equal to the Planck length ℓ_P . In a similar way the counting of the updating steps corresponds to time, with the conversion factor given by the Planck time τ_P . Specifically as a framework for QFT the quantum systems are field evaluations on the lattice, and a priori it can be taken Bosonic or Fermionic.

After reviewing the one-dimensional Dirac automaton, in Sect. II we show how the automaton recovers precisely the Dirac dynamics in the limit of small masses and momenta. Then in Sect III we present an analytical approximation method for evaluating the automaton evolution for single-particle states smooth in momentum and with limited bandwidth—the typical quantum states of field theory. In this way we derive a momentum-dependent Schrödinger equation, which works very well in all regimes, including ultrarelativistic and Planckian. We compare computer simulations with the analytic approximation, and provide the leading order corrections to the Dirac equation. After discussing thought experiments for falsifying the existence of the automaton at the Planck scale in Sect.IV, we conclude the paper with future perspectives.

II. THE ONE-DIMENSIONAL DIRAC AUTOMATON

In this section we review the one-dimensional Dirac automaton of Ref. [29], which is the focus of the present paper. Then we show how the Dirac dynamics is recovered for low momenta and masses.

A. Derivation of the Dirac Automaton

In QFT the unitary evolution of a field $\psi(x)$ with Λ internal degrees of freedom is given by

$$\psi(t+1) = U^\dagger \psi(t) U, \quad \psi(x) = \{\psi_\lambda(x)\}_{\lambda=1,\dots,\Lambda}. \quad (1)$$

The QCA corresponding to the one-step update of the field can be described by a unitary matrix \mathbf{U} acting linearly on the field operator ψ

$$\psi(t+1) = \mathbf{U} \psi(t), \quad \psi(t) := \begin{pmatrix} \dots \\ \psi(x, t) \\ \psi(x+1, t) \\ \dots \end{pmatrix} \quad (2)$$

where we use the symbols $x \in \mathbb{Z}$ and $t \in \mathbb{Z}$ for the adimensional numbering of the lattice sites and time steps respectively. A pictorial representation of the automaton \mathbf{U} is shown in Fig.1 where the light cones depict the local structure of the evolution, and at every site $x \in \mathbb{Z}$ of the lattice there are Λ systems corresponding to the internal components of the field.

When the lattice dimension is one, the most general translational invariant QCA with next-neighbouring interaction is given by

$$\mathbf{U} = \mathbf{R}S + \mathbf{L}S^\dagger + \mathbf{M}, \quad (3)$$

where S denotes the shift operator

$$S\psi(x) := \psi(x+1), \quad (4)$$

and \mathbf{R} , \mathbf{L} and \mathbf{M} are $\Lambda \times \Lambda$ matrixes which do not depend on the lattice site, due to translation invariance. The unitarity of \mathbf{U} implies

$$\begin{aligned} \mathbf{R}\mathbf{R}^\dagger + \mathbf{L}\mathbf{L}^\dagger + \mathbf{M}\mathbf{M}^\dagger &= I, \\ \mathbf{M}\mathbf{R}^\dagger + \mathbf{L}\mathbf{M}^\dagger &= 0, \quad \mathbf{L}\mathbf{R}^\dagger = 0. \end{aligned} \quad (5)$$

We now derive the Dirac automaton as the minimal-dimension QCA, satisfying the following requirements

- i. Unitarity of the evolution;
- ii. Homogeneity of the interaction topology;
- iii. Invariance under time-reversal $t \mapsto -t$;
- iv. Invariance under parity $x \mapsto -x$;
- v. Minimal dimension for a non-identical evolution.

The first two assumptions are already contained in the definition itself of QCA. Assumptions iii and iv are the symmetries of the pure topology of the causal network (in Fig. 2), corresponding to considering the network as undressed. The next-neighbouring interaction is not an assumption by itself, since it is always possible to reduce to such a case by grouping a periodic pattern of the network into a single node of the automaton. Therefore, the only assumption is the minimality one v. In equations, assumptions iii and iv correspond to

$$\mathbf{T}\mathbf{U}\mathbf{T}^\dagger = \mathbf{U}^\dagger, \quad (6)$$

$$\mathbf{P}\mathbf{U}\mathbf{P}^\dagger = \mathbf{R}S^\dagger + \mathbf{L}S + \mathbf{M}, \quad (7)$$

where \mathbf{T} is the anti-unitary operator associated to the time reversal transformation, and \mathbf{P} is the unitary operator of the lattice reflection. Notice that $\mathbf{P}\mathbf{U}\mathbf{P}^\dagger$ is the same as \mathbf{U} with S exchanged with S^\dagger . For $\Lambda = 1$ the only translational invariant QCA satisfying parity invariance is the identical one $\mathbf{U} = I$. Next, we have the case $\Lambda = 2$. Eq. (7) shows that \mathbf{R} and \mathbf{L} are unitarily equivalent, whence, from Eq (5) it follows that they are both rank one. Thus we can choose the basis where

$$\mathbf{R} = \begin{pmatrix} a_1 & a_2 \\ 0 & 0 \end{pmatrix}, \quad \psi(x) := \begin{pmatrix} \psi_R(x) \\ \psi_L(x) \end{pmatrix}, \quad (8)$$

naming the two components of the field ψ_R and ψ_L *right* and *left* modes. We now require \mathbf{P} and \mathbf{T} to be represented in such basis as

$$\mathbf{P} = \begin{pmatrix} 0 & 1 \\ 1 & 0 \end{pmatrix}, \quad \mathbf{T} = \mathbf{C} \begin{pmatrix} 0 & 1 \\ 1 & 0 \end{pmatrix}, \quad (9)$$

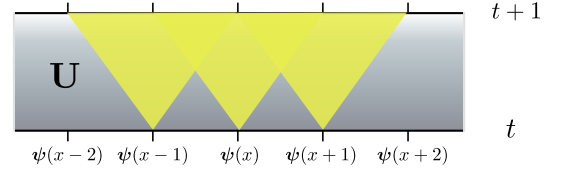


FIG. 1: Illustration of a one-dimensional quantum cellular automaton unitary step. Each site of the lattice x corresponds to a quantum field evaluation $\psi(x)$. The field operator at site x interacts with the field $\psi(x \pm 1)$ at neighbouring sites. In the case of the Dirac automaton the field operator has two components (see text).

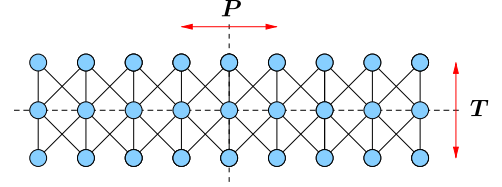


FIG. 2: Schematic of the three time steps causal network corresponding to a one-dimensional quantum cellular automaton with next-neighbouring interaction. The topology of the network is left invariant by the mappings $t \mapsto -t$ and $x \mapsto -x$ and the dynamics of the automaton is assumed to be time reversal (\mathbf{T}) and parity (\mathbf{P}) invariant (see Eqs. (6) and (7)).

where \mathbf{C} is the anti-unitary operator denoting complex conjugation in the representation (8). With this choice of basis the parity invariance (7), which implies $\mathbf{P}\mathbf{R}\mathbf{P}^\dagger = \mathbf{L}$ and $\mathbf{P}\mathbf{M}\mathbf{P}^\dagger = \mathbf{M}$, gives

$$\mathbf{R} = \begin{pmatrix} a_1 & a_2 \\ 0 & 0 \end{pmatrix}, \quad \mathbf{L} = \begin{pmatrix} 0 & 0 \\ a_2 & a_1 \end{pmatrix}, \quad \mathbf{M} = \begin{pmatrix} a_3 & a_4 \\ a_4 & a_3 \end{pmatrix} \quad (10)$$

with $a_i \in \mathbb{C}$ for $i = 1, \dots, 4$. From the time time-reversal invariance (6), that is $\mathbf{T}\mathbf{R}\mathbf{T}^\dagger = \mathbf{L}^\dagger$ and $\mathbf{T}\mathbf{M}\mathbf{T}^\dagger = \mathbf{M}^\dagger$, it follows $a_2 = a_3 = 0$. Finally, using the unitarity of \mathbf{U} (5) we get $|a_1|^2 + |a_4|^2 = 1$ and $\Re(a_1 \bar{a}_4) = 0$ which, up to a global phase, give the unique automaton

$$\mathbf{U} = \begin{pmatrix} nS & -im \\ -im & nS^\dagger \end{pmatrix}, \quad n^2 + m^2 = 1. \quad (11)$$

The constants n and m in the last equation can be chosen positive (the relative sign corresponds to take the left-mode redefined with a minus sign). The unitarity constraint $n^2 + m^2 = 1$ in Eq. (11) forces the parameter m to be $m \in [0, 1]$. As we will see in the following, m plays the role of an adimensional inertial mass, whereas n is the inverse of a refraction index of vacuum. Thus, the inertial mass of the field is bounded from above [29], as mentioned in the introduction. In the digital-analog conversion from the automaton to the usual dimensional Dirac equation, we take the Planck length ℓ_P and the Planck time τ_P as conversion factors for space and time respectively, whereas the mass conversion factor is taken equal to the Planck mass m_P . The maximal speed of

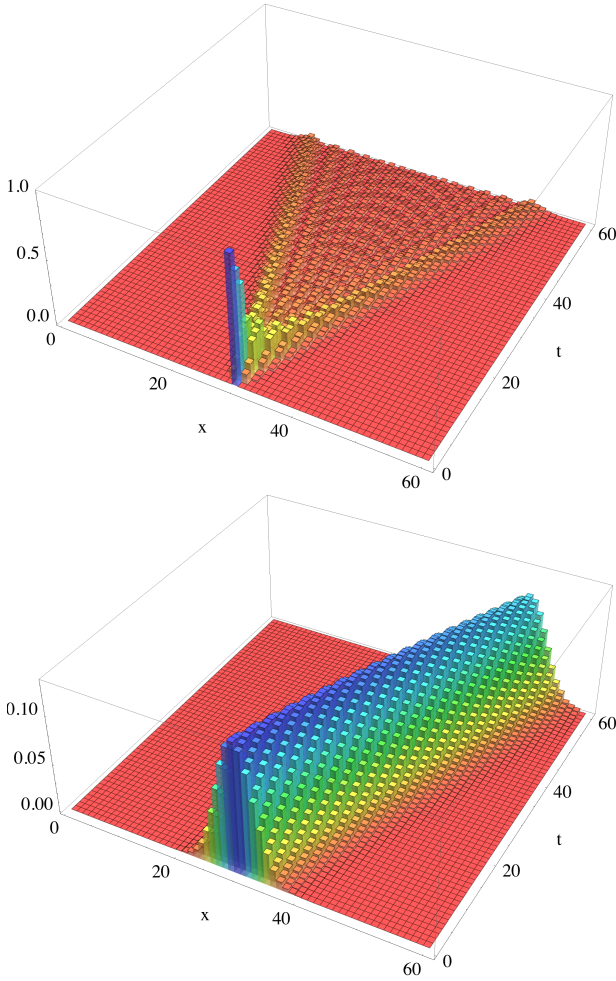


FIG. 3: (Colors online) The automaton ($m = 0.92$) evolution for a localized state (top) and a smooth state (bottom). The localized state cannot be described by QFT, whereas the smooth state is a typical QFT state (for more details see text). The localized state is given by $|30\rangle \otimes \frac{1}{\sqrt{2}}(1, 1)$. The smooth state is given by $\sum_x g(x)e^{ikx}|x\rangle \otimes |+\rangle_k$ with $g(x)$ Gaussian with mean value $x_0 = 30$ and width $\hat{\sigma} = 3$. $|+\rangle_k$ is a one particle eigenstate (21) of the Dirac automaton with momentum $k = 0.3\pi$ (see text).

local-state propagation in the dimensional case is then $c = \ell_P/\tau_P$, corresponding to the speed of light. ℓ_P , τ_P , and m_P are three fundamental universal constants defining the measure for dimensions $[L]$ $[T]$ $[M]$, and from them one can derive any other universal constant, e.g. $\hbar = m_P \ell_P c$ [30]. The automaton for $m = 0$ corresponds to the Weyl equation, and will be refereed as Weyl automaton.

In Fig. 3 we give two computer evaluations of the automaton evolution for a localized state not describable by QFT, and for a smooth state of the kind used in QFT (for more details see the following). The same Dirac automaton of (11) is also derived in Ref. [32], by recovering the Weyl automaton for $d = 3$ as the unique minimal QCA, whereas the Dirac automaton is then the only possible

local coupling of two Weyl automata (the only possible automata that can be coupled are a pair of reciprocally inverse automata). In this way one obtains a two-spinor automaton, which for $d = 1$ splits into two identical automata of the form given in Eq (11). Originally the automaton of (11) has been derived heuristically as the one describing the free flow of quantum information [29].

B. Recovering the Dirac dynamics

Here we show how the Dirac QCA (11) recovers, for low momenta and masses, the dynamics of the Dirac equation which is

$$i\hbar\partial_t\psi(x,t) = \begin{pmatrix} -i\hbar c\partial_x & mc^2 \\ mc^2 & i\hbar c\partial_x \end{pmatrix} \psi(x,t). \quad (12)$$

The digital version of the equation corresponds to using adimensional x , t , and m (corresponding to Planck units), with $\hbar = c = 1$. For convenience, as usual in the literature ([39–43]), we study the dynamics of the automaton in the momentum representation. For the field operator we have

$$\psi(k) := \frac{1}{\sqrt{2\pi}} \sum_{x \in \mathbb{Z}} e^{-ikx} \psi(x), \quad k \in [-\pi, \pi], \quad (13)$$

where with little abuse of notation we utilize the variable name k to denote the Fourier transform of any function of x . Notice that the automaton model is naturally band-limited $k \in [-\pi, \pi]$ ($k \in [-\pi/\ell_P, \pi/\ell_P]$ in usual units) and periodic in momenta due to the discreteness of the lattice. Correspondingly, for the unitary matrix \mathbf{U} in Eq. (11) we have

$$\mathbf{U} = \int_{-\pi}^{\pi} dk \mathbf{U}(k), \quad \mathbf{U}(k) = \begin{pmatrix} ne^{ik} & -im \\ -im & ne^{-ik} \end{pmatrix}. \quad (14)$$

By taking a real power of the unitary matrix, we define an abstract Hamiltonian that describes the automaton evolution for continuous times, interpolating between time-steps, namely $\mathbf{U}^t = \exp(-i\mathbf{H}t)$. Upon diagonalizing the matrix $\mathbf{U}(k)$ in Eq. (14), one obtains

$$\mathbf{H} = \int_{-\pi}^{\pi} dk \mathbf{H}(k), \quad (15)$$

$$\mathbf{H}(k) = \frac{\omega}{\sin(\omega)} \begin{pmatrix} -n \sin(k) & m \\ m & n \sin(k) \end{pmatrix}, \quad (16)$$

where $\omega(k, m)$ is the dispersion relation of the automaton

$$\omega(k, m) = \arccos(\sqrt{1 - m^2} \cos(k)). \quad (17)$$

Notice that the Hamiltonian \mathbf{H} is unphysical, as is unphysical the continuous process between two following time-steps. Indeed, one could easily see that the Hamiltonian (15) involves interactions between all systems, including those very far apart (the “local” Hamiltonian

corresponding to the finite-difference form of the usual Dirac field Hamiltonian is given by the imaginary part of \mathbf{U} [28]).

We now expand $\mathbf{H}(k)$ near $k = 0$ and $m = 0$, in order to recover the Dirac equation for the quantum field, along with the first corrections. One has

$$\mathbf{H}(k) = \sum_{i,j=0}^{\infty} \frac{1}{i!j!} \left. \frac{\partial \mathbf{H}(k)}{\partial k^i \partial m^j} \right|_{k,m=0} k^i m^j \quad (18)$$

and collecting all terms with the same overall order in m and k , we find

$$\mathbf{H}(k) = \mathbf{H}_D(k) + \frac{m}{3} \begin{pmatrix} mk & \frac{1}{2}(k^2 + m^2) \\ \frac{1}{2}(k^2 + m^2) & -mk \end{pmatrix} + O(m^p k^q) \quad \text{where } p+q=5 \quad (19)$$

where $\mathbf{H}_D(k)$ is the adimensional Dirac Hamiltonian of Eq. (12) in the momentum representation

$$\mathbf{H}_D(k) = \begin{pmatrix} -k & m \\ m & k \end{pmatrix}. \quad (20)$$

The Hamiltonian (20) identifies the parameters k and m of the automaton with the momentum and the mass of the Dirac field, respectively. With the automaton operating at the Planck scale the maximal mass must coincide with the Planck mass m_P . Remembering the value m_P in usual units $m_P = 2.17651(13) \times 10^{-8} \text{kg} = 1.2209 \times 10^{28} \text{eV}/c^2$, a particle having rest mass $100 \text{GeV}/c^2$ as e.g. the Higg's boson corresponds to an adimensional mass $m \approx 10^{-17}$ (for the electron and the proton one would have $m_e \approx 10^{-23}$ and $m_p \approx 10^{-19}$, respectively). Similarly a momentum of $10^{20} \text{eV}/c$, the highest ever observed for Ultra-High Energy Cosmic Rays (UHECRs, see for example [44]), corresponds in Planckian units to $k_{CR} \approx 10^{-8}$ (a high energy momentum of 1Tev in reachable in a LHC experiments corresponds to $k_{LHC} \approx 10^{-16}$). Therefore, the relativistic approximation works very well in particle physics experiments.

C. Dispersion relation

The eigenvalues and the eigenvectors of the unitary matrix $\mathbf{U}(k)$ in Eq. (14) are given by

$$u_k(s) = e^{-is\omega}, \quad |s\rangle_k := \frac{1}{\sqrt{2}} \begin{bmatrix} \sqrt{1-sv} \\ s\sqrt{1+sv} \end{bmatrix}, \quad s = \pm, \quad (21)$$

in terms of the automaton dispersion relation (17) and the group velocity $v = \partial_k \omega$.

In Fig. 4 the automaton dispersion relation ω is compared with the Dirac one

$$\omega_D := \omega_D(k, m) = \sqrt{k^2 + m^2}. \quad (22)$$

The dispersion relations show an overlap vs k around $k = 0$ for small m corresponding to the typical particle-physics regime. Analytically, the leading term correction

to the Dirac dispersion is given by

$$\omega = \omega_D \left(1 - \frac{m^2}{6} \frac{k^2}{k^2 + m^2} \right). \quad (23)$$

Notice that the smallest non zero value of the mass $m = 0.3$ reported in Fig. 4 is huge compared to any particle mass, and still is possible to find a sector in the momentum space around $k = 0$ where the automaton dispersion relation well overlaps the Dirac one. This means that for m sufficiently small it is possible to fix a cutoff in the momenta $|k| \leq \bar{k} < \pi$ such that in that regime the Dirac automaton and the usual Dirac evolution are very similar. The zone-border value $k = \pi$ describes the Planck-scale behaviour, whereas smaller k correspond to look at the automaton at larger scales. We emphasize the conceptual difference between the large scale limit analyzed here $|k| \leq \bar{k} < \pi$ with $\ell = l_P$, $\tau = t_P$, and the continuum limit $\ell \rightarrow 0$, $\tau \rightarrow 0$ considered in Refs. [24, 25].

D. Particle states

The QCA automaton \mathbf{U} generally operates on the vector field ψ which describes an arbitrary number of particles. The vacuum state for the automaton is defined as the state $|\Omega\rangle$ such that

$$\psi_s(k)|\Omega\rangle = 0 \quad \forall s = \pm, \quad \forall k \in [-\pi, \pi]. \quad (24)$$

Up to now, we have not specified the nature Fermionic/Bosonic of the field, and indeed the same automaton could be used to describe both cases (along with anyons and parastatistics): the relation spin-statistics will be considered for the the automaton with $d = 3$ space-dimensions [32]. Here we will focus only on the Fermionic case of anticommuting field. A N -particle state can be obtained by acting with the field operator on the vacuum as follows

$$|N, \mathbf{k}, \mathbf{s}\rangle = \left(\prod_{i=1}^N \psi_{s_i}^\dagger(k_i) \right) |\Omega\rangle. \quad (25)$$

Specifically, for $N = 1$ particle eigenstates of \mathbf{U} , we write

$$\psi_s^\dagger(k)|\Omega\rangle = |s\rangle_k |k\rangle, \quad (26)$$

whereas for $N = 2$ we have

$$\psi_{s_1}^\dagger(k_1) \psi_{s_2}^\dagger(k_2) |\Omega\rangle = |s_1\rangle_{k_1} |s_2\rangle_{k_2} |k_1, k_2\rangle \quad (27)$$

where $|k_1, k_2\rangle = -|k_2, k_1\rangle$, and so forth for $N > 2$. The corresponding eigenvalues of the (logarithm of) \mathbf{U} are

$$\omega(N, \mathbf{k}, \mathbf{s}) = \sum_{i=1}^N s_i \omega(k_i, m). \quad (28)$$

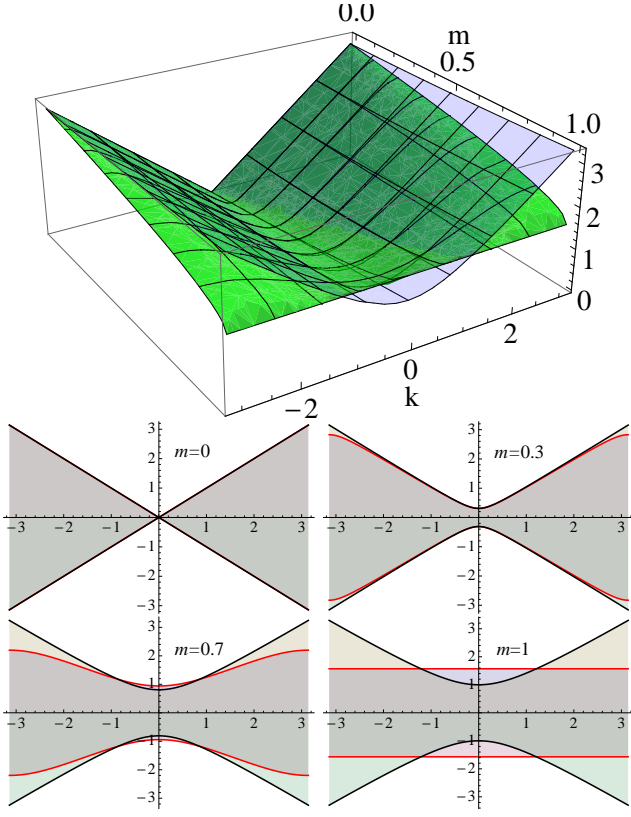


FIG. 4: (Colors online) Comparison between the dispersion relations $\omega(k, m)$ of the Dirac automaton and of the Dirac equation, in Eqs (17) and (22), respectively. In the top figure the dispersion relation is plotted versus the adimensional mass $m \in [0, 1]$ and momentum $k \in [-\pi, \pi]$ ($m = 1$ corresponds to the Planck mass). The green surface represent the automaton, whereas the blue the Dirac one. In the bottom figures $\omega(k, m)$ is plotted versus k for four values of m (the red line corresponds to the automaton, whereas the black one is the Dirac's). We can see that the two dispersion relations coincide for small masses and momenta, and the larger the mass the smaller the overlap region around $k = 0$.

III. THE QUANTUM-FIELD LIMIT OF THE AUTOMATON

The ultimate aim of this approach to QFT is clearly the connection to phenomenology. In the last section we will provide a bound from an optimization over all possible experimental setups of the probability of discriminating between the Dirac automaton and usual Dirac evolution. This is a powerful result, both from the theoretical and the phenomenological point of view, since it allows to verify the theoretical discriminability between the two theories, giving insights on the most suitable experimental scenario where searching for violations of the usual Dirac evolution. However, the huge class of experimental setups considered in the derivation of the bound includes also configurations non realizable with the present technology.

In this section we explore the behaviour of the Dirac

QCA for the one-particle states of quantum field theory. We consider initial states whose momentum distribution is smoothly peaked around some k_0 , namely

$$|\psi(0)\rangle = \int_{-\pi}^{\pi} \frac{dk}{\sqrt{2\pi}} g(k, 0) |s\rangle_k |k\rangle, \quad s = \pm, \quad (29)$$

where $g(k, 0) \in C_0^\infty[-\pi, \pi]$ is a smooth function satisfying the bound

$$\frac{1}{2\pi} \int_{k_0-\sigma}^{k_0+\sigma} dk |g(k, 0)|^2 \geq 1 - \epsilon, \quad \sigma, \epsilon > 0. \quad (30)$$

where the two-component vector $|s\rangle_k$ is defined in Eq. (21).

At time t and in the position representation, the state in Eq. (29) can be written as

$$\begin{aligned} |\psi(t)\rangle &= \sum_x |\psi(x, t)\rangle |x\rangle \\ |\psi(x, t)\rangle &:= e^{i(k_0 x - s \omega_0 t)} |\phi(x, t)\rangle \\ |\phi(x, t)\rangle &:= \int_{-\pi}^{\pi} \frac{dk}{\sqrt{2\pi}} e^{i(Kx - s \Omega(k, m)t)} g(k, 0) |s\rangle_k \end{aligned} \quad (31)$$

where we posed

$$\begin{aligned} K &= k - k_0, \\ \Omega(k, m) &= \omega(k, m) - \omega_0, \quad \omega_0 = \omega(k_0, m). \end{aligned} \quad (32)$$

A. The k -dependent Schrödinger equation

It is convenient to take x, t to be real-valued continuous variable by extending the Fourier transform in Eq. (31) to real x, t . We derive the integral in Eq. (31) with respect to t , and expand Ω vs k around k_0 up to the second order. Then, taking the resulting derivatives with respect to x out of the integral (using the dominated derivative theorem), we obtain the following k -dependent Schrödinger equation with drift

$$i\partial_t |\tilde{\phi}(x, t)\rangle = s \left(iv \frac{\partial}{\partial x} - \frac{1}{2} D \frac{\partial^2}{\partial x^2} \right) |\tilde{\phi}(x, t)\rangle, \quad (33)$$

with the drift constant v and the diffusion constant D depending on k and m as follows

$$v := \sqrt{\frac{1 - m^2}{1 + m^2 \cot^2(k_0)}}, \quad (34)$$

$$D := \frac{\sqrt{1 - m^2} m^2 \cos(k_0)}{(\sin^2(k_0) + m^2 \cos^2(k_0))^{\frac{3}{2}}}, \quad (35)$$

and with the identification of the initial condition

$$|\tilde{\phi}(x, 0)\rangle = |\phi(x, 0)\rangle. \quad (36)$$

The drift and diffusion coefficients are obtained as derivatives of the dispersion relation as $v = \omega_{k_0}^{(1)}$ and $D = \omega_{k_0}^{(2)}$, where

$$\omega_{k_0}^{(n)} = \left. \frac{\partial^n \omega(k, m)}{\partial k^n} \right|_{k_0}. \quad (37)$$

For $|\psi(x, 0)\rangle$ satisfying Eq. (30), Eq. (33) provides the approximation of the state of the particle $|\tilde{\psi}(x, t)\rangle = e^{i(k_0 x - s \omega_0 t)} |\tilde{\phi}(x, t)\rangle$, corresponding to

$$|\tilde{\psi}(t)\rangle = \int_{-\pi}^{\pi} \frac{dk}{\sqrt{2\pi}} e^{-is(\omega_0 + vk - \frac{1}{2} Dk^2)t} g(k, 0) |s\rangle_k |k\rangle. \quad (38)$$

B. Accuracy of the approximation

The accuracy of this approximation can be quantified in terms of the parameters σ and ϵ of the initial state by evaluating (see Appendix A) the overlap between the states (31) and (38)

$$|\langle \tilde{\psi}(t) | \psi(t) \rangle| \geq 1 - \epsilon - \gamma \sigma^3 t - \mathcal{O}(\sigma^5)t. \quad (39)$$

where

$$\gamma = \frac{\omega_{k_0}^{(3)}}{2\pi} \int_{k_0 - \sigma}^{k_0 + \sigma} dk |g(k, 0)|^2.$$

Notice that the choice of smooth function $g(k, t)$ corresponds to a two-component vector $|\psi(x, t)\rangle$ that is Schwartz on the real line, as for the field of QFT. We are thus evaluating the asymptotic field-limit of the QCA.

The approximation (38) works well in all regimes, namely for any mass m and momentum k . We can test the accuracy of the approximation by comparing $|\tilde{\psi}(x, t)\rangle$ with the automaton simulation for given initial state. In Fig. 5 we show an example in the Planckian ultrarelativistic regime. Here the Schwartz-class field state (29) is a superposition of Hermite functions (the polynomials $H_j(x)$ multiplied by the Gaussian) peaked around a very high momentum $k_0 = 3\pi/10$ and for inertial mass $m = 0.6$. The mean value moves at the group velocity given by the drift coefficient v . One can notice how the approximation remains accurate even for small position spreads of few Planck lengths. For a spread $\hat{\sigma}$ of the order of a Fermi as in a typical particle physics scenario, the time t needed for a significant departure would be comparable to many universe life-times.

C. The relativistic regime

In the relativistic regime for $k, m \ll 1$ and $k/m \gg 1$, the k -dependent Schrödinger equation (33) approaches the Dirac equation. The leading order and the corrections to the drift and diffusion coefficients introduced by the automaton evolution are

$$v = \frac{k}{\sqrt{k^2 + m^2}} \left(1 - \frac{1}{3} m^2 + \frac{1}{6} \frac{m^2 k^2}{k^2 + m^2} \right), \quad (40)$$

$$D = \frac{m^2}{\sqrt{(k^2 + m^2)^3}} \left(1 + \frac{1}{3} m^2 k^2 - \frac{1}{2} \frac{m^2 k^4}{k^2 + m^2} \right). \quad (41)$$

The leading order in v and D correspond to the Dirac equation.

D. The non relativistic regime

In the non relativistic regime, $k, m \ll 1$ and $k/m \ll 1$ the usual Schrödinger drift and diffusion coefficients are recovered with the following corrections

$$v = \frac{k}{m} \left(1 + \frac{1}{3} m^2 \right), \quad (42)$$

$$D = \frac{1}{m} \left(1 + \frac{5}{6} k^2 \right). \quad (43)$$

Notice that the leading terms are just the usual group-velocity and diffusion coefficient of the Schrödinger equation.

IV. TESTING THE QUANTUM AUTOMATON

In this section we consider an elementary thought experiment for testing the granularity of the quantum automaton based on particle flying-time, and compare it with the theoretical optimal in-principle testing. As we will see, the latter needs time duration of the order of an hour, whereas the former requires a time comparable to the age of the universe. Other experiments could be devised e.g. using quantum interferometry and/or ultra-cold atoms as in Refs. [19–22]: these will be considered in a forthcoming publication on the three-dimensional Dirac automaton.

A. Discrimination via particle flying-time

The k -dependent Schrödinger equation (33) along with the leading terms in the relativistic and non relativistic regimes in subsections III C and III D provide a unique analytic tool for evaluating the macroscopic evolution of the automaton, which otherwise would not be computable in practice. As a thought experiment for an experimental falsification of a quantum automaton evolution at the Planck scale we consider a measurement of fly time of a particle. As for order of magnitude, we consider numerical values corresponding to ultra high energy cosmic rays (UHECR) [44]).

Consider then a proton UHECR with $m_p \approx 10^{-19}$ and momentum peaked around $k_{CR} \approx 10^{-8}$ in Planck units, with a spread σ . We ask what is the minimal time t_{CR} for observing a complete spatial separation between the trajectory predicted by the cellular automaton model and the one described by the usual Dirac equation. Thus we require the separation between the two trajectories to be greater than $\hat{\sigma} = \sigma^{-1}$ the initial proton's width in the position space. Notice that UHECR still belong to the relativistic regime $m_p, k_{CR} \ll 1$ (see Subsect. III C), where the automaton well approximates the usual Dirac evolution.

We describe the state evolution of the wavepacket of the proton using the k -dependent Schrödinger equation

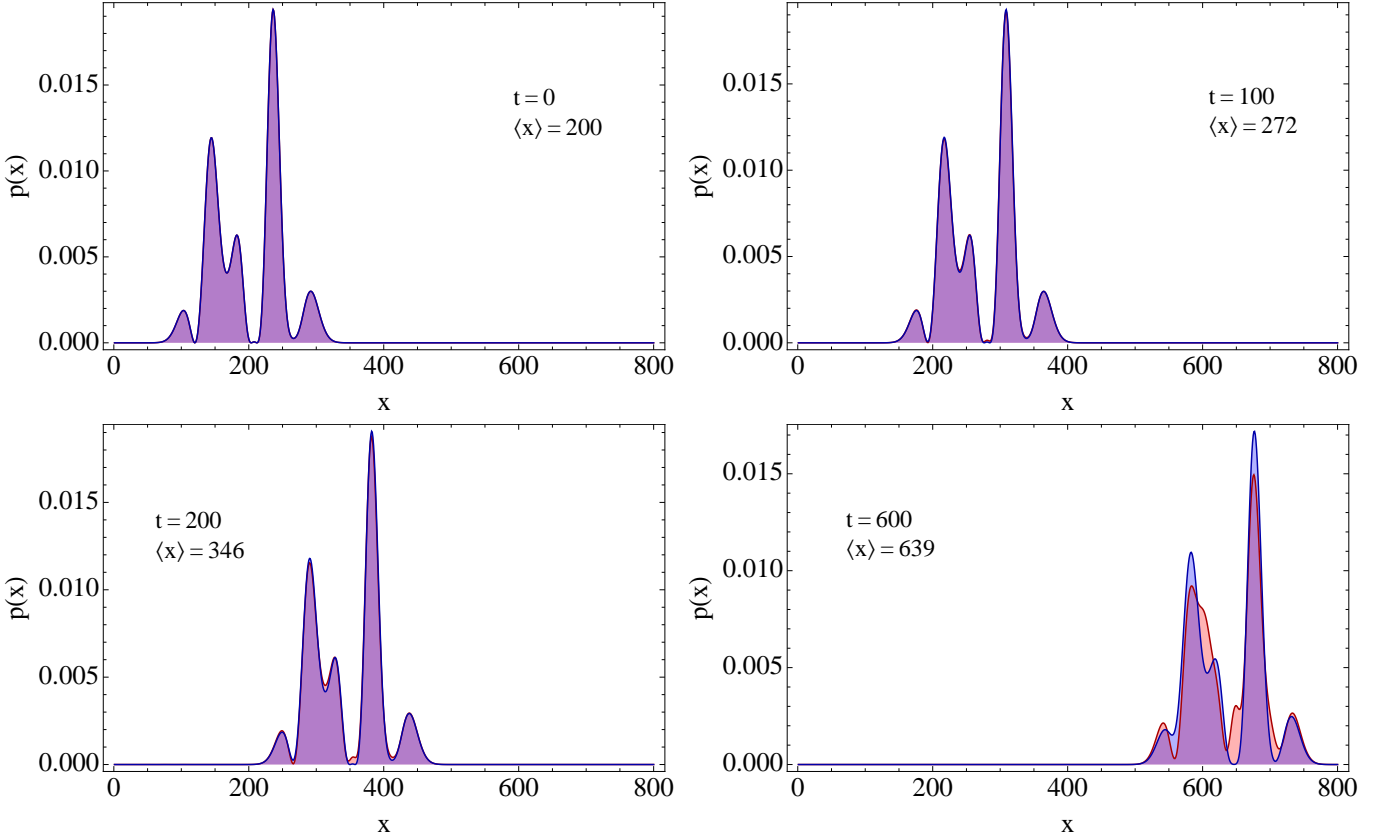


FIG. 5: (Colors online) Test of the approximation (38) of the Dirac automaton evolution Eq. (11) in one space dimension. The approximation corresponds to the quantum-field asymptotic behaviour. Here the state (29) of the Schwartz class as in QFT, is a superposition of Hermite functions (the polynomials $H_j(x)$ multiplied by the Gaussian) peaked around momentum $k_0 = 3\pi/10$, specifically $|\psi(x,0)\rangle = \mathcal{A}e^{ik_0x} \sum_{j \in \mathbb{N}} c_j e^{-x^2/4\hat{\sigma}^2} H_j(x/2\hat{\sigma})|+\rangle_{k_0}$ where $\hat{\sigma} = \sigma^{-1} = 20$ is the position variance corresponding to momentum variance σ , and the nonvanishing terms are $c_0 = \sqrt{1/3}$, $c_2 = \sqrt{4/9}$, $c_7 = \sqrt{2/9}$. The automaton mass is $m = 0.6$. The momentum and mass parameters are in the Planckian ultrarelativistic regime. In the picture we show a comparison at four different times $t = 0$, $t = 100$, $t = 200$ and $t = 600$ between the automaton probability distribution $|\psi(x,t)|^2$ (in red) and the solution of the Schrödinger equation (33) $|\tilde{\psi}(x,t)|^2$ (in blue). The drift and diffusion coefficients are respectively $v = 0.73$ and $D = 0.31$. The mean value moves at the group velocity given by the drift coefficient v . The approximation remains accurate even for position spread $\hat{\sigma} = 20$ Planck lengths. According to Eq. (39) one has significant deviations for $t \approx \gamma\sigma^3$, which is $t = 600$ in the present case. However, a reasonable spread $\hat{\sigma}$ in a typical particle physics scenario is the Fermi length $\hat{\sigma} \approx 10^{20}$, that would need a time t comparable to many universe life-times to introduce a significant error. The ϵ error in Eq. (39) can be taken very small by considering $n\sigma$ instead of σ in Eq. (29). For Gaussian states it is enough to consider 3σ to get $\epsilon \approx 10^{-3}$.

(33) with initial Gaussian state. The Dirac evolution is very precisely given by the Schrödinger equation (33) just the leading-order terms in Eqs. (40) and (41), whereas the automaton is described in this regime by the full expansion. The time required to have a separation $\hat{\sigma}$ between the automaton and the Dirac particle can be easily calculated using the power expansion in Eq. (40)

$$t \approx \hat{\sigma} \left| \frac{6\sqrt{(k^2 + m^2)^3}}{m^2 k^2 (2m^2 + k)} \right|, \quad (44)$$

which, since it is $m_p/k_{CR} \ll 1$ further simplifies as follows

$$t_{CR} \approx 6 \frac{\hat{\sigma}}{m_p^2}. \quad (45)$$

In order to be visible the separation $\hat{\sigma}$, the overall broadening $\hat{\sigma}_{br}(t)$ of the two packets must be much smaller than $\hat{\sigma}$. Using Eq. (41) one has

$$\begin{aligned} \hat{\sigma}_{br}(t) &= \hat{\sigma} \left(\sqrt{1 + \left(\frac{D}{2\hat{\sigma}^2} t \right)^2} + \sqrt{1 + \left(\frac{D_D}{2\hat{\sigma}^2} t \right)^2} - 2 \right) \\ &\approx 2\hat{\sigma} \left(\sqrt{1 + \frac{m_p^4}{4\hat{\sigma}^4 k_{CR}^6} t^2} - 1 \right) \end{aligned}$$

where $D_D = m^2(k^2 + m^2)^{-3/2}$ and we used $m_p/k_{CR} \ll 1$. Using Eq. (45) we see that $\hat{\sigma} \gg \hat{\sigma}_{br}$ when

$$\hat{\sigma} \gg (k_{CR})^{-3} = 10^{22} \text{ Planck lengths} = 10^2 \text{ fm}, \quad (46)$$

a physical result, considering a reasonable width for the proton packet of the order of a Fermi or bigger. With $\hat{\sigma} = 10^2 \text{ fm}$ the flying time request for complete separation between the two trajectories is

$$t_{CR} \approx 6 \times 10^{60} \text{ Planck times} \approx 10^{17} s, \quad (47)$$

comparable with the universe age. In Subsec. IV B we will evaluate the minimal theoretical time required for discriminating perfectly between the automaton and the Dirac evolution using UHECR.

B. Theoretically optimal discrimination

The problem of discriminating optimally between two different dynamics is what is usually refereed to as “discrimination between two black boxes”. An experimentalist is given a black box that can be either the automaton (box A) or Dirac equation (box D) with equal probability, and is asked to guess which box. The box discrimination is a two-outcome experiment, with outcomes A and D. The correct answer is given with some probability, and the challenge is to minimize the probability error (wrong guess)

$$p_e = \frac{1}{2} [p(A|D) + p(D|A)] \quad (48)$$

where $p(X|Y)$ is the probability of getting outcome X when the black box is Y. We want now to minimize p_e over all the possible experiments. The optimal discrimination between the two black boxes is a special case of discrimination between quantum channels, namely the discrimination between the two unitary evolutions described by U_A and U_D . Generally, the optimization between quantum channels needs entangled states [45], but for the case of two unitary evolutions with a single copy of each box, the optimal error probability \bar{p}_e is given by [45]

$$\bar{p}_e = \frac{1}{2} - \frac{1}{2} \|U_A - U_D\|. \quad (49)$$

However, such a probability with no restriction on the input states would be vanishingly small in the case of large dimension for the Hilbert space. We thus consider the physical bounds on the number of particles $N \leq \bar{N}$ and their momentum $k \leq \bar{k}$. In such case the old Helstrom’s result gives [46]

$$\bar{p}_e = \frac{1}{2} - \frac{1}{2} \sup_{\rho \in \mathcal{T}_{\bar{k}, \bar{N}}} \|U_A \rho U_A^\dagger - U_D \rho U_D^\dagger\|_1, \quad (50)$$

where $\mathcal{T}_{\bar{k}, \bar{N}}$ denotes the set of physically restricted states

$$\rho \in \mathcal{T}_{\bar{k}, \bar{N}} \text{ iff } \text{Tr}[\rho N_{\bar{k}}] = \text{Tr}[\rho P_{\bar{N}}] = 0 \quad (51)$$

where $P_{\bar{N}}$ is the projector on the $N > \bar{N}$ -particles sector and $N_{\bar{k}}$ is the operator that counts the number of particles with momentum $|k| > \bar{k}$, i.e $N_{\bar{k}} =$

$\int_{|k| > \bar{k}} dk \psi^\dagger(k) \psi(k)$. In Appendix B we evaluate a lower bound for the optimal probability of error, which is given by

$$\bar{p}_e \geq \frac{1}{2} - \frac{1}{2} \sqrt{1 - \cos^2(g(\bar{k}, m, \bar{N}, t))} \quad (52)$$

where

$$\begin{aligned} g(\bar{k}, m, \bar{N}, t) &:= \bar{N} \arccos(\cos(\bar{\alpha}t) - \bar{\beta}) \\ \bar{\alpha} &:= \max_{k \in \{0, \bar{k}\}} |\omega_D - \omega|, \\ \bar{\beta} &:= \max_{k \in \{0, \bar{k}\}} \left| \frac{1}{2} \left(1 - vv_D - \sqrt{(1 - v^2)(1 - v_D^2)} \right) \right| \end{aligned} \quad (53)$$

and v (see Eq. (34)) and $v_D = k/\sqrt{k^2 + m^2}$ the automaton and the Dirac drift coefficients.

A simplified version of the bound in the typical particle physics regime, namely $k, m \ll 1$ is obtained by expanding in series the function g in Eq. (53) near $m = \bar{k} = 0$. Truncating the expansion at the leading order and neglecting a small constant term we have

$$g(m, \bar{k}, \bar{N}, t) \approx \frac{1}{6} m^2 \bar{k} \bar{N} t. \quad (54)$$

By putting $\bar{p}_e = 0$, corresponding to $g(m, \bar{k}, \bar{N}, t) = \pi/2$, we obtain the minimum time required for discriminating perfectly between the automaton and the Dirac evolution

$$t_{min}(m, \bar{k}, \bar{N}) \approx 3\pi \frac{1}{m^2 \bar{k} \bar{N}}. \quad (55)$$

Notice that this is an in-principle optimal result, without any specification of the actual apparatus needed to achieve it. For a proton UHECR with $\bar{k} = k_{CR} \approx 10^{-8}$ we have

$$t_{min}(m_p, k_{CR}, 1) \approx 3\pi 10^{46} \text{ Planck times} \approx 10^3 s, \quad (56)$$

which is many orders of magnitude smaller than the time in the flying-time experiment of Subsect. IV A.

V. CONCLUSIONS

In this paper, based only on the parity and time-reversal invariance and without requiring Lorentz covariance, we have derived a QCA that describes the Dirac evolution. The automaton extends the Dirac field theory to the Planck and ultrarelativistic scales. The Dirac equation is recovered for small m and k .

We have provided a technique to derive an analytical approximation of the evolution of the automaton in terms of a momentum-dependent Schrödinger equation. The approximation works very well for quantum states typical of QFT having limited bandwidth in momentum, and gives precise estimation of the automaton behaviour in all regimes, including ultrarelativistic and Planckian.

We have then presented a thought experiment for testing the automaton using a fly-time discrimination between the automaton state and the Dirac one, for the

typical UHECR scale. However, this leads to a time-duration of the experiment that is comparable to the universe life-time. We have then considered the in-principle discrimination between the Dirac and the automaton evolution, optimizing over all measurement apparata and preparation available according to quantum theory, and providing the general discrimination formula. For the case of UHECR we got an experiment duration of the order of 10^3 s.

The present preliminary analysis of the QCA extension of QFT to the Planck scale has proved very effective in evaluating experimentable phenomenology, and this motivates pursuing investigation of more general QCAs, with possible correspondence to the theory of fundamental interactions, and including a theory quantum gravity. This, in consideration of the simplicity of the automaton, of the principles at the basis of the QCA, and of all motivations that we expressed in the introduction, namely the fact that the Lorentz covariance is not assumed a priori but is recovered as emergent, the fact that the QCA is quantum *ab-initio*, the fact that it doesn't suffer violations of causality, and is free from all the problems arising from the continuum.

Next steps in the QCA research will be the Dirac Equation in $3 + 1$ dimensions [32], and the corresponding k -dependent Schrödinger equation. The $3 + 1$ dimensional case is particularly relevant in view of the spin-statistics connection. At least for the Dirac automaton, also in $3 + 1$ dimensions the automaton is derived with minimal assumptions, as in the present case, and the usual Dirac equation with two spinors emerges for small m and k . As regards gauge-invariance the QCA has a very natural embedded quantum gauge-invariance, through the choice of a local unitary operator on each system of the quantum lattice, and this opens a route to the interacting QFTs. One of the problems that are still open is the possibility of achieving the automaton by qubits on the lattice, a problem that dates back to the famous work of Feynman [34]. In the present 1-dimensional case the simple Jordan-Wigner transform achieves the transformation from local qubits to nonlocal Fermi fields [29]. The extension to higher dimensions of the Jordan-Wigner is straightforward, however, it is still not clear if it is possible to map local field interactions to local interactions between qubits. It seems that a possible solution requires auxiliary fields of the Majorana kind [28, 47, 48]. The possible solution of the Feynman problem may shade light on the intimate difference between the Fermionic and the Bosonic natures.

VI. ACKNOWLEDGMENTS

We thank Paolo Perinotti for interesting discussions and suggestions. A. Bisio and A. Tosini acknowledge useful discussion with Daniel Reitzner.

Appendix A: Derivation of Eq. (39)

Here we evaluate the overlap between the exact automaton evolution $|\psi(t)\rangle$ and the k -dependent Schrödinger approximation $|\tilde{\psi}(t)\rangle$

$$\begin{aligned} |\langle \tilde{\psi}(t) | \psi(t) \rangle| &= \left| \int_{-\pi}^{\pi} \frac{dk}{2\pi} e^{-i(\omega_{k_0}^{(3)} k^3 + \mathcal{O}(k^4))t} |g(k, 0)|^2 \right| \geq \\ &\geq \left| \frac{1}{2\pi} \int_{k_0-\sigma}^{k_0+\sigma} dk e^{-i(\omega_{k_0}^{(3)} k^3 + \mathcal{O}(k^4))t} |g(k, 0)|^2 \right| + \\ &- \left| \frac{1}{2\pi} \int_{|k-k_0| \geq \sigma} dk e^{-i(\omega_{k_0}^{(3)} k^3 + \mathcal{O}(k^4))t} |g(k, 0)|^2 \right| \geq \\ &\left| 1 - it \frac{\omega_{k_0}^{(3)} \sigma^3}{2\pi} \int_{k_0-\sigma}^{k_0+\sigma} dk |g(k, 0)|^2 - \mathcal{O}(\sigma^5)t \right| - \epsilon \geq \\ &\geq 1 - \epsilon - \gamma \sigma^3 t - \mathcal{O}(\sigma^5)t \end{aligned}$$

with the constant $\gamma = \frac{\omega_{k_0}^{(3)}}{2\pi} \int_{k_0-\sigma}^{k_0+\sigma} dk |g(k, 0)|^2$.

Appendix B: Proof of the bound (52)

In this appendix we detail the proof of the bound (52) in Section IV B which provides the probability of optimal error probability in discriminating the Dirac automaton and the usual Dirac evolution. The discrimination experiment can have a generic duration t and the unitary operators to be discriminated are explicitly given by

$$\begin{aligned} \mathbf{U}^t(k) &= \exp(-i\mathbf{H}(k)t) = \\ &= \begin{pmatrix} \cos(\omega t) + i \frac{\sin(\omega t)}{\omega} a & -ib \frac{\sin(\omega t)}{\omega} \\ -ib \frac{\sin(\omega t)}{\omega} & \cos(\omega t) - i \frac{\sin(\omega t)}{\omega} a \end{pmatrix} \end{aligned} \quad (\text{B1})$$

$$\begin{aligned} \mathbf{U}_D^t(k) &= \exp(-i\mathbf{H}_D(k)t) = \\ &= \begin{pmatrix} \cos(\lambda t) + i \frac{\sin(\lambda t)}{\lambda} k & -im \frac{\sin(\lambda t)}{\lambda} \\ -im \frac{\sin(\lambda t)}{\lambda} & \cos(\lambda t) - i \frac{\sin(\lambda t)}{\lambda} k \end{pmatrix}. \end{aligned} \quad (\text{B2})$$

as can be easily verified by direct computation using the Hamiltonians in Eqs. (14) and (20). The proof of the bound (52) goes through the following three Lemmas.

Lemma 1 *Let $\mathbf{U}_D^t(k)$ and $\mathbf{U}^{t\dagger}(k)$ be defined according to Eqs. (B1),(B2) and let us define $\mathbf{V}(k, t) = \mathbf{U}_D^t(k) \mathbf{U}^{t\dagger}(k)$ Let $e^{i\mu(k, m, t)}$ be an eigenvalue of $\mathbf{V}(k, t)$. Then the following bound holds:*

$$\cos(\mu(k, m, t)) \geq \cos(\alpha t) - \beta \quad (\text{B3})$$

where

$$\begin{aligned} \alpha(k, m) &:= \omega_D - \omega \\ \beta(k, m) &:= \frac{1}{2} \left(1 - v v_D - \sqrt{(1 - v^2)(1 - v_D^2)} \right). \end{aligned} \quad (\text{B4})$$

Proof. Since both $U_D^t(k)$ and $U^{t\dagger}(k)$ are $SU(2)$ matrices, we have that $V(k, t)$ is an $SU(2)$ matrix and its eigenvalues must be of the form $e^{i\mu(k, m, t)}$ and $e^{-i\mu(k, m, t)}$. This implies the equality $\cos(\mu(k, m, t)) = \frac{1}{2} \text{Tr}[V(k, t)]$ which by direct computation gives

$$\cos(\mu(k, m, t)) = \left(1 - \frac{\beta}{2}\right) \cos(\alpha t) + \frac{\beta}{2} \cos(\gamma t) \quad (\text{B5})$$

where α and β are defined accordingly with Eq. (B4) and $\gamma := \omega + \omega_D$. Finally, from Eq. (B5) one has the bound $\cos(\mu(k, m, t)) \geq \cos(\alpha t) - \beta$ ■

The second Lemma shows the monotonicity of the two functions α, β in Lemma 1:

Lemma 2 Let $\alpha(k, m)$ and $\beta(k, m)$ be defined as in Eq. (B4) and $0 \leq \bar{k} < \pi$ Then we have

$$\begin{aligned} \bar{\alpha} &:= \max_{k \in [-\bar{k}, \bar{k}]} |\alpha| = \max_{k \in \{0, \bar{k}\}} |\alpha| \\ \bar{\beta} &:= \max_{k \in [-\bar{k}, \bar{k}]} |\beta| = \max_{k \in \{0, \bar{k}\}} |\beta| \end{aligned} \quad \forall m \in [0, 1]. \quad (\text{B6})$$

Proof. Since both ω and ω_D are even function of k , from Eq. (B4) we have that also α and β are even function of k . For this reason we can restrict to $k \in [0, \bar{k}]$. The equality (B6) can be proved by showing that α and β are nondecreasing function of k for $k \in [0, \bar{k}]$.

Since $\partial_k \alpha = v_D - v$, clearly $v_D^2 - v^2 \geq 0$ for $k \in [0, \pi)$ implies $\partial_k \alpha \geq 0$ in the same interval. By direct computation one can verify that

$$(v_D)^2 - (v)^2 = \frac{x(k, m)}{y(k, m)} \quad (\text{B7})$$

$$x(k, m) := k^2 - \sin^2(k)(1 - m^2) \quad (\text{B8})$$

$$y(k, m) := (k^2 + m^2)(\sin^2(k) + m^2 \cos^2(k)). \quad (\text{B9})$$

Clearly we have $y(k, m) \geq 0$ and since $k \geq \sin(k)$ for $0 \leq k < \pi$, the thesis is proved.

Again the monotonicity of β for $k \in [0, \pi)$ follows from $\partial_k \beta \geq 0$ in the same interval. By elementary computation we have

$$\partial_k \beta = x(k, m)y(k, m)z(k, m) \quad (\text{B10})$$

$$x(k, m) := \frac{m^2}{\omega_D \sin^2(\omega)} \quad (\text{B11})$$

$$y(k, m) := (n \sin(k) - k) \quad (\text{B12})$$

$$z(k, m) := \frac{n \cos(k)}{\sin^2(\omega)} - \frac{1}{\omega_D^2} \quad (\text{B13})$$

Clearly $x(k, m)y(k, m) \leq 0$ for $k \in [0, \pi)$ and we just have to verify that $z(k, m) \leq 0$ in that interval, namely

$$m^2 \cos^2(k) + \sin^2(k) - n \cos(k) \omega_D^2 \geq 0. \quad (\text{B14})$$

The last equation is clearly satisfied for $k \in [\pi/2, \pi]$ therefore we restrict to $k \in [0, \pi/2]$. This allows to divide the left side of Eq. (B14) by $\cos(k)$ achieving

$$m^2 \cos(k) + \frac{\sin^2(k)}{\cos(k)} - n \omega_D^2 \geq 0 \quad (\text{B15})$$

which is satisfied if

$$w(k, m) := m^2 \cos(k) + \sin^2(k) - n \omega_D^2 \geq 0. \quad (\text{B16})$$

It is easy to see that, for any $m \in [0, 1]$, we have $(\partial_k^{(i)} w(k, m))_{k=0} = 0$ for $i = 0, 1$, while $\partial_k^{(2)} w(k, m) \geq 0$ for any $k \in [0, \pi/2]$, which gives the monotonicity of β . ■

Lemma 3 Let $0 \leq \bar{k} < \pi$, N be a positive integer number, and $\bar{\alpha}, \bar{\beta}$ be defined as in Eq. (B6). If $\bar{\beta} \leq 1 - \cos(\frac{\pi}{2N})$ and $t \leq f(\bar{k}, m, N)$ where

$$f(\bar{k}, m, N) := \frac{\arccos(\cos(\frac{\pi}{2N}) + \bar{\beta})}{\bar{\alpha}} \quad (\text{B17})$$

then

$$N\mu(k, m, t) \leq g(\bar{k}, m, N, t) \leq \frac{\pi}{2} \quad (\text{B18})$$

where $g(\bar{k}, m, N, t) := N \arccos(\cos(\bar{\alpha} t) - \bar{\beta})$.

Proof. The conditions $t \leq f(\bar{k}, m, N)$ and $\bar{\beta} \leq 1 - \cos(\frac{\pi}{2N})$ imply

$$\begin{aligned} 0 &\leq \bar{\alpha} t \leq \arccos(\cos(\frac{\pi}{2N}) + \bar{\beta}) \Rightarrow \\ &\Rightarrow 1 \geq \cos(\bar{\alpha} t) - \bar{\beta} \geq \cos(\frac{\pi}{2N}) \Rightarrow \\ &\Rightarrow \cos(\alpha t) - \beta \geq \cos(\bar{\alpha} t) - \bar{\beta} \geq \cos(\frac{\pi}{2N}). \end{aligned} \quad (\text{B19})$$

By exploiting the bound (B3) into Eq. (B19) we have

$$\begin{aligned} \cos(\mu(k, m, t)) &\geq \cos(\bar{\alpha} t) - \bar{\beta} \geq \cos(\frac{\pi}{2N}) \Rightarrow \\ &\Rightarrow N\mu(k, m, t) \leq N \arccos(\cos(\bar{\alpha} t) - \bar{\beta}) \leq \frac{\pi}{2}. \end{aligned} \quad (\text{B20})$$

■

We are now ready to prove the bound (52)

Proposition 1 Let U^t and U_D^t be the unitary evolution given by the Dirac QCA and by the Dirac equation respectively. If the hypothesis of Lemma 3 hold we have

$$\sup_{\rho \in \mathcal{T}_{\bar{k}, N}} \|(U^t \rho U^{t\dagger} - U_D^t \rho U_D^{t\dagger})\|_1 \leq \sqrt{1 - \cos^2(g(\bar{k}, m, N, t))}. \quad (\text{B21})$$

Proof. First we notice that thanks to the convexity of the trace distance we can without loss of generality consider ρ to be pure. If ρ is a pure state $|\chi\rangle\langle\chi|$ the trace distance becomes $\sqrt{1 - |\langle\chi|U^t U_D^{t\dagger}|\chi\rangle|^2} = \sqrt{1 - |\langle\chi|V(t)|\chi\rangle|^2}$. If we expand $|\chi\rangle$ on a basis of eigenstates of V , i.e. $|\chi\rangle = \sum_{N, \mathbf{k}, \mathbf{s}} \sqrt{p_{N, \mathbf{k}, \mathbf{s}}} |N, \mathbf{k}, \mathbf{s}\rangle$, we have

$$\begin{aligned} |\langle\chi|V(t)|\chi\rangle| &= \left| \sum_{N, \mathbf{k}, \mathbf{s}} p_{N, \mathbf{k}, \mathbf{s}} \exp\left(i \sum_{j=0}^{\bar{N}} s_j \mu(k_j, m, t)\right) \right| \geq \\ &\geq \left| \sum_{N, \mathbf{k}, \mathbf{s}} p_{N, \mathbf{k}, \mathbf{s}} \cos\left(\sum_{j=0}^{\bar{N}} s_j \mu(k_j, m, t)\right) \right|. \end{aligned} \quad (\text{B22})$$

By exploiting the bound (B18) into Eq. (B22) we have

$$\left| \sum_{N, \mathbf{k}, \mathbf{s}} p_{N, \mathbf{k}, \mathbf{s}} \cos \left(\sum_{j=0}^{\bar{N}} s_j \mu(k_j, m, t) \right) \right|^2 \geq \cos^2(g(\bar{k}, m, \bar{N}, t))$$

which finally implies

$$\sqrt{1 - |\langle \chi | V(t) | \chi \rangle|^2} \leq \sqrt{1 - \cos^2(g(\bar{k}, m, \bar{N}, t))}.$$

Inserting the bound (B21) into Eq. (50) we finally have the bound (52).

-
- [1] M. Kuhlmann, in *The Stanford Encyclopedia of Philosophy*, edited by E. N. Zalta (<http://plato.stanford.edu/archives/win2012/entries/quantum-field-theory/>, 2012), winter 2012 ed.
 - [2] T. Y. Cao and S. S. Schweber, *Synthese* **97**, 33 (1993).
 - [3] P. Teller, *An interpretive introduction to quantum field theory* (Princeton Univ Pr, 1997).
 - [4] S. Y. Auyang, *How is quantum field theory possible?* (Oxford University Press, USA, 1995).
 - [5] T. Y. Cao, *Conceptual foundations of quantum field theory* (Cambridge Univ Pr, 2004).
 - [6] W. N. Cottingham and D. A. Greenwood, *An introduction to the standard model of particle physics* (Cambridge University Press, 2007).
 - [7] H. Reeh and S. Schlieder, *Il Nuovo Cimento* (1955-1965) **22**, 1051 (1961).
 - [8] G. N. Fleming and J. Butterfield, in *From physics to philosophy*, edited by J. Butterfield and C. Pagonis (Cambridge University Press, 1999), pp. 108–165.
 - [9] B. Thaller, *The Dirac Equation* (New York, NY (United States); Springer-Verlag, 1992).
 - [10] A. Connes and J. Lott, *Nuclear Physics B-Proceedings Supplements* **18**, 29 (1991).
 - [11] H. S. Snyder, *Physical Review* **71**, 38 (1947).
 - [12] C. Rovelli and L. Smolin, *Nuclear Physics B* **8**, 80 (1990).
 - [13] C. Rovelli and L. Smolin, *Nuclear Physics B* **442**, 593 (1995).
 - [14] A. Ashtekar, C. Rovelli, and L. Smolin, *Physical Review Letters* **69**, 237 (1992).
 - [15] L. Bombelli, J. Lee, D. Meyer, and R. D. Sorkin, *Physical Review Letters* **59**, 521 (1987).
 - [16] G. Amelino-Camelia, *Int. Journ. of Modern Physics D* **11**, 35 (2002).
 - [17] G. Amelino-Camelia and T. Piran, *Physical Review D* **64**, 036005 (2001).
 - [18] J. Maguiejo and L. Smolin, *Physical Review D* **67**, 044017 (2003).
 - [19] M. Moyer, *Scientific American* (2012).
 - [20] C. Hogan, *Physical Review D* **85** (2012).
 - [21] I. Pikovski, M. R. Vanner, M. Aspelmeyer, M. Kim, and C. Brukner, *Nature Physics* **331**, 393 (2012).
 - [22] G. Amelino-Camelia, C. Laemmerzahl, F. Mercati, and G. M. Tino, *Physical Review Letters* **103**, 171302 (2009).
 - [23] T. Nakamura, *Journal of mathematical physics* **32**, 457 (1991).
 - [24] I. Bialynicki-Birula, *Physical Review D* **49**, 6920 (1994).
 - [25] D. A. Meyer, *Journal of Statistical Physics* **85**, 551 (1996).
 - [26] J. Yepez, *Quantum Information Processing* **4**, 471 (2006).
 - [27] G. M. D’Ariano, *CP1232 Quantum Theory: Reconsideration of Foundations 5* (arXiv:1001.1088) **3** (2010).
 - [28] G. M. D’Ariano, *Advances in Quantum Theory*, AIP Conf. Proc. 1327 p. 7 (2011).
 - [29] G. M. D’Ariano, *Phys. Lett. A* **376** (2011), [arXiv:1012.0756 (2010)].
 - [30] G. M. D’Ariano, (arXiv:1211.2479) (2012).
 - [31] G. M. D’Ariano, *Il Nuovo Saggiatore* **28**, 13 (2012).
 - [32] G. M. D’Ariano and P. Perinotti, unpublished (2012).
 - [33] J. von Neumann and A. W. Burks, *Theory of self-reproducing automata* (University of Illinois Press, 1966).
 - [34] R. P. Feynman, *International journal of theoretical physics* **21**, 467 (1982).
 - [35] G. Grossing and A. Zeilinger, *Complex Systems* **2**, 197 (1988).
 - [36] B. Schumacher and R. F. Werner, Arxiv preprint quant-ph/0405174 (2004).
 - [37] P. Arrighi, V. Nesme, and R. Werner, *Journal of Computer and System Sciences* **77**, 372 (2011).
 - [38] D. Gross, V. Nesme, H. Vogts, and R. F. Werner, *Communications in Mathematical Physics* pp. 1–36 (2012).
 - [39] A. Ambainis, E. Bach, A. Nayak, A. Vishwanath, and J. Watrous, in *Proceedings of the thirty-third annual ACM symposium on Theory of computing* (ACM, 2001), pp. 37–49.
 - [40] P. L. Knight, E. Roldán, and J. E. Sipe, *journal of modern optics* **51**, 1761 (2004).
 - [41] G. J. Valcárcel, E. Roldán, and A. Romanelli, *New Journal of Physics* **12**, 123022 (2010).
 - [42] A. Ahlbrecht, H. Vogts, A. H. Werner, and R. F. Werner, *Journal of Mathematical Physics* **52**, 042201 (2011).
 - [43] D. Reitzner, D. Nagaj, and V. Bužek, *Acta Physica Slovaca. Reviews and Tutorials* **61**, 603 (2011).
 - [44] M. Takeda, N. Hayashida, K. Honda, N. Inoue, K. Kadota, F. Kakimoto, K. Kamata, S. Kawaguchi, Y. Kawasaki, N. Kawasumi, et al., *Physical Review Letters* **81**, 1163 (1998).
 - [45] G. M. D’Ariano, P. Lo Presti, and M. G. A. Paris, *Physical Review Letters* **87**, 270404 (2001).
 - [46] C. W. Helstrom, *Quantum detection and estimation theory*, vol. 84 (Academic press New York, 1976).
 - [47] F. Verstraete and J. I. Cirac, *Journal of Statistical Mechanics: Theory and Experiment* **2005**, P09012 (2005).
 - [48] G. M. D’Ariano and A. Tosini, unpublished (2012).